Immunology
The Journal of cells, molecules, systems and technologies

British Society for immunology

IMMUNOLOGY ORIGINAL ARTICLE

Analyses of phenotypic and functional characteristics of CX3CR1-expressing natural killer cells

Isabell Hamann,[1] Nadine Unterwalder,[2] Astrid E. Cardona,[3] Christian Meisel,[2] Frauke Zipp,[4] Richard M. Ransohoff[5] and Carmen Infante-Duarte[1]

[1]*Experimental and Clinical Research Centre, Charité – Universitätsmedizin Berlin and Max Delbrück Centre for Molecular Medicine, Berlin, Germany,* [2]*Institut für Medizinische Immunologie, Charité – Universitätsmedizin Berlin, Berlin, Germany,* [3]*Department of Biology, the University of Texas at San Antonio, San Antonio, TX, USA,* [4]*Department of Neurology, University Medical Centre, Johannes Gutenberg, University, Mainz, Germany, and* [5]*Neuroinflammation Research Center, Lerner Research Institute, Cleveland Clinic, Cleveland, OH, USA*

doi:10.1111/j.1365-2567.2011.03409.x
Received 27 August 2010; revised 21 December 2010; accepted 6 January 2011.
Correspondence: Dr C. Infante-Duarte, Neuroscience Research Centre, Charité – Universitätsmedizin Berlin, Charitéplatz 1, 10117 Berlin, Germany. Email: carmen.infante@charite.de
Senior author: Carmen Infante-Duarte

Summary

We previously demonstrated a correlation between the frequency of CX3CR1-expressing human natural killer (NK) cells and disease activity in multiple sclerosis and showed that CX3CR1^{high} NK cells were more cytotoxic than their CX3CR1$^{neg/low}$ counterparts. Here we aimed to determine whether human NK cell fractions defined by CX3CR1 represent distinct subtypes. Phenotypic and functional NK cell analyses revealed that, distinct from CX3CR1^{high}, CX3CR1$^{neg/low}$ NK cells expressed high amounts of type 2 cytokines, proliferated robustly in response to interleukin-2 and promoted a strong up-regulation of the key co-stimulatory molecule CD40 on monocytes. Co-expression analyses of CX3CR1 and CD56 demonstrated the existence of different NK cell fractions based on the surface expression of these two surface markers, the CX3CR1^{neg} CD56^{bright}, CX3CR1^{neg} CD56^{dim} and CX3CR1^{high} CD56^{dim} fractions. Additional investigations on the expression of NK cell receptors (KIR, NKG2A, NKp30 and NKp46) and the maturation markers CD27, CD62L and CD57 indicated that CX3CR1 expression of CD56^{dim} discriminated between an intermediary CX3CR1^{neg} CD56^{dim} and fully mature CX3CR1^{high} CD56^{dim} NK cell fractions. Hence, CX3CR1 emerges as an additional differentiation marker that may link NK cell maturation with the ability to migrate to different organs including the central nervous system.

Keywords: chemokines; CX3CR1; natural killer cell maturation; natural killer cell phenotypes; natural killer cells.

Introduction

The chemokine receptor CX3CR1 is the only member of the CX3C subfamily.[1] Its exclusive ligand fractalkine (CX3CL1) exists as a transmembrane glycoprotein as well as in soluble form. CX3CR1 is expressed on monocytes, dendritic cells, natural killer (NK) cells, as well as cytotoxic and also activated helper T cells, preferentially on T helper type 1 (Th1) -like cells, but not on B cells.[2–4] CX3CL1 and its receptor are implicated in several human pathological conditions including atherosclerosis,[5–7] age-related macular degeneration,[8,9] allograft rejection,[10,11] rheumatic diseases[12,13] and cytomegalovirus-related vascular endothelial damage.[14] In rodent models of brain pathologies, the CX3CR1/CX3CL1 axis has been related to both pathological leucocyte migration into the central nervous system (CNS)[15,16] as well as neuroprotective mechanisms.[17,18] In experimental autoimmune encephalomyelitis, a mouse model of multiple sclerosis, CX3CL1/CX3CR1 interactions govern the selective recruitment of potential protective NK cells into the brain.[19] Multiple sclerosis is an inflammatory demyelinating disease of the CNS with an unclear pathogenesis.[20] A hallmark of the disease is the abundant infiltration of leucocytes into

Abbreviations: APC, allophycocyanin; CFSE, carboxyfluorescein succinimidyl ester; CNS, central nervous system; c.p.m., counts per minute; GM-CSF, granulocyte–macrophage colony-stimulating factor; IFN, interferon; IL-2, interleukin-2; NK cell, natural killer cell; neg, negative; PBMC, peripheral blood mononuclear cell; PE, phycoerythrin; PerCP, peridinin chlorophyll protein; TGF, transforming growth factor; Th1, T helper type 1; TNF, tumour necrosis factor.

the CNS, which leads to demyelination as well as axonal and neuronal damage.[21] The role of NK cells in multiple sclerosis development is not established. However, it has become evident that, apart from their potential contribution to tissue injury, NK cells may be involved in the regulation of the autoimmune attack,[22,23] as suggested by the findings of Huang *et al.* [19] In line with these findings,[19] we correlated the frequency of circulating CX3CR1-positive NK cells with disease activity in patients with multiple sclerosis.[24] We also reported that NK cells with a high expression of CX3CR1 were more cytotoxic than NK cells showing a negative/low receptor expression,[24] indicating that CX3CR1 expression may dissect functionally different NK cell subsets. To investigate this and further contribute to the elucidation of the role of NK cells and CX3CR1 in neuroinflammation, we determined the phenotypic and functional characteristics of CX3CR1$^{neg/low}$ and CX3CR1^{high} expressing NK cells.

Material and methods

Culture medium and reagents

Cells were cultured in serum-free AIM-V medium (Gibco-Invitrogen, Karlsruhe, Germany), complete medium (RPMI-1640 supplemented with 2 mM L-glutamine, 100 U/ml penicillin, 100 μg/ml streptomycin, 10% fetal calf serum, and 1% HEPES) or AB medium [RPMI-1460 supplemented with 2 mM L-glutamine, 100 U/ml penicillin, 100 μg/ml streptomycin, 5% AB serum (Lonza, Walkersville, MD), and 0·5% Ciprobay (Bayer Vital GmbH, Leverkusen, Germany)]. Interleukin-2 (IL-2) was purchased from Hoffmann-La Roche (Basel, Switzerland); IL-12 and transforming growth factor-β1 (TGF-β1; from R&D, Minneapolis, MN); IL-15 and Fractalkine from PreproTech (Rocky Hill, NJ); IL-21 from Biosource (Camarillo, CA) and IL-18 as well as anti-human CX3CR1 (phycoerythrin-labelled) from MBL (Nagoya, Japan). Rat serum was purchased from DakoCytomation (Hamburg, Germany) and human Fc fragment was purchased from Calbiochem (Merck Chemicals Ltd., Darmstadt, Germany). The antibody mix containing anti-CD3 fluorescein isothiocyanate (FITC)/anti-CD16CD56 phycoerythrin (PE), the anti-human antibodies CD3 peridinin chlorophyll protein (PerCP), CD4 PerCP, CD16 FITC/Pacific Blue, CD25 allophycocyanin (APC), CD14 APC, CD40 FITC and HLA-DR FITC, CD62L APC, the isotype control IgG2b PE and streptavidin APC were purchased from Becton-Dickinson (Heidelberg, Germany). Biotin anti-human CD11c, CD86 PE, CD56 FITC and biotin CD27 were purchased from eBioscience (San Diego, CA). The APC-labelled anti-human CD57, KIR2DL1/2DS1, KIR3DL1/3DL2, NKp30 and NKp46 were purchased from Miltenyi Biotech (Bergisch-Gladbach, Germany). The antibody against human KIR3DL1/3DS1 was purchased from Beckman Coulter GmbH (Krefeld, Germany) and anti-human KIRDL2/2DS2/2DL3 and NKG2A were from R&D.

Isolation of PBMCs and preparation of NK cells and monocytes

Peripheral blood mononuclear cells (PBMCs) were isolated from buffy coats by density gradient centrifugation (Percoll, Nycomed Pharma, Roskilde, Denmark) according to the manufacturer's instructions. The NK cells were negatively sorted from freshly isolated PBMCs using the NK isolation kit (Miltenyi Biotech). Monocytes were positively sorted from freshly isolated PBMCs using CD14 MicroBeads (Miltenyi Biotech) according to the manufacturer's instructions. The purity of enriched NK cells and monocytes was confirmed using flow cytometric analysis and was always > 90%.

Flow cytometry analysis

For the determination of the activation levels of the different CX3CR1-expressing subpopulations of NK cells, freshly isolated PBMCs were washed and incubated with anti-CD3 PerCP, anti-CD16 FITC, anti-CD25 APC and anti-CX3CR1 PE antibodies for 20 min at room temperature. After washing, cells were analysed on a FACSCanto.

For the analysis of CX3CR1 expression on whole NK cells and phenotypic characterization of CX3CR1^{high} and CX3CR1$^{neg/low}$ NK cells, freshly isolated PBMCs were washed and stained with antibodies against CD3, CD56, CD16, CX3CR1 and CD62L, CD57, CD27, NKG2A, panKIR (KIR2DL1/2DS1/2DL2/2DS2/2DL3/3DL1/3DL2/3DS1), NKp30 and NKp46. For the analysis of monocytes from the NK cell : monocyte co-culture, cells were blocked with Fc fragments for 10 min and subsequently stained with antibodies against human CD14, CD11c, CD40, CD86 and HLA-DR according to standard procedures. Flow cytometric analyses were performed on a FACSCanto. Data were analysed using the FlowJo software (Tree Star, Inc., Ashland, OR).

Quantitative real-time RT-PCR

Magnetically sorted NK cells were stained with a PE-labelled anti-human CX3CR1 antibody and sorted into CX3CR1$^{neg/low}$-expressing and CX3CR1^{high}-expressing fractions on a FACSAria Cell Sorting System (Becton-Dickinson, Heidelberg, Germany). Sorted NK cells were then adjusted to $1{\cdot}6 \times 10^6$ per ml and incubated in 100 ng/ml PMA and 1 μg/ml ionomycin for 4 hr. Cells were then harvested and total RNA was isolated using the RNeasy Mini kit (Qiagen, Hilden, Germany) according to the manufacturer's instructions. RNA was then transcribed to cDNA with random hexamers using TaqMan Reverse Transcription Reagents (Applied Biosystems, Darmstadt, Germany). Quantitative real-time RT-PCR was performed on the ABI

PRISM 7000 Sequencing Detection System (Applied Biosystems) using the qPCR Mastermix Plus (Eurogentec, Seraing, Belgium). The comparative threshold method (comparative *C*t method) was used to quantify the results obtained by real-time RT-PCR. Data were normalized to the corresponding housekeeping gene *beta-actin*. Primers and probes (FAM-TAMRA-labelled) that were used are listed in Table 1. The probes were labelled with the reporter dye carboxyfluorescein (FAM) at the 5′-end and with the quencher dye tetramethylrhodamin (TAMRA) at the 3′-end (Table 1). For granulocyte–macrophage colony-stimulating factor (GM-CSF), TaqMan Gene Expression Assays (Applied Biosystems) were used.

For determination of the CX3CR1 expression on NK cells in the presence of cytokines, purified NK cells were cultured in serum-free media in IL-2, IL-12, IL-15, IL-18, IL-21, or TGF-β, respectively, for 20–22 hr (concentrations are listed in Table 2). Afterwards, cells were harvested, washed, and total RNA was isolated as mentioned above. The *CX3CR1* mRNA levels were assessed by quantitative real-time RT-PCR and normalized to the housekeeping gene *beta-actin*. The primers and FAM-TAMRA-labelled probe for *CX3CR1* are listed in Table 1. All samples were run in duplicates.

Proliferation assays

Ninety-six-well flat-bottom plates were coated with 1 μg/ml anti-CD3, incubated for 2 hr at 37° and washed afterwards with PBS. CD4-positive T cells from freshly isolated PBMCs were positively selected using CD4 MicroBeads (Miltenyi) and incubated with 2·5 μM carboxyfluorescein succinimidyl ester (CFSE) in RPMI (Gibco, Invitrogen GmbH, Darmstadt, Germany) supplemented with 1% HEPES for 10 min at 37° in 5% CO_2. The NK cells from the same donor were negatively selected using the NK cell isolation Kit (Miltenyi). Purity of enriched cells was assessed and was always > 90%. Thereafter NK cells were FACS-sorted into $CX3CR1^{neg/low}$-expressing and $CX3CR1^{high}$-expressing NK cells. Ratios of effector (NK cells) to target (T) cells ranging from 1 : 12·5 to 1 : 50 were plated together with aCD28 (2·5 μg/ml) and incubated for 72 hr at 37° in 5% CO_2. Cells were then harvested and stained with an antibody against human CD4 conjugated with PerCP. Percentage of proliferating CD4-positive cells was analysed by flow cytometry.

For determination of the IL-2 response of NK cells, presorted $CX3CR1^{neg/low}$-expressing and $CX3CR1^{high}$-expressing NK cells were incubated in a 96-well flat bottom plate without or with IL-2 (100 U/ml) for 72 hr at 37° in 5% CO_2. [^{3}H]Thymidine (Amersham, Braunschweig, Germany) was then added at a dose of 0·5 μCi to each well. After 18 hr, incorporation of radioactivity was measured in counts per minute (c.p.m.) with a Microbeta β counter (Wallac ADL, Freiburg, Germany).

For the analysis of NK cell proliferation using CFSE, freshly isolated NK cells were stained with CD56, CD16, CD3 and CX3CR1 and subsequently FACS-sorted into $CX3CR1^{neg}$ $CD56^{bright}$, $CX3CR1^{neg}$ $CD56^{dim}$ and $CX3CR1^{high}$ $CD56^{dim}$ NK cell fractions. Sorted NK cell fractions (1×10^6 cells/ml) were incubated with CFSE as described above for T cells. Labelled cells were plated in 96-well plates and stimulated with and without 100 U/ml IL-2 at 37° in

Table 1. Primers and probes for real time RT-PCR

Name	Primer	Sequence 5′→3′	Company
Beta-actin	Forward	GGC ACC CAG CAC AAT GAA G	TIB MOLBIOL, Germany
	Reverse	GCC GAT CCA CAC GGA GTA CT	TIB MOLBIOL, Germany
	Probe	TCA AGA TCA TTG CTC CTC CTG AGC GC	Microsynth, Germany
Interleukin-5	Forward	ATA GCC AAT GAG ACT CTG AGG ATT C	TIB MOLBIOL, Germany
	Reverse	TCC ACA GTA CCC CCT TGC A	TIB MOLBIOL, Germany
	Probe	TCA GGG AAT AGG CAC ACT GGA GAG TCA AAC	MWG GmbH, Germany
Interleukin-10	Forward	CAA GTT GTC CAG CTG ATC CTT CAT	MWG GmbH, Germany
	Reverse	GGC AAC CTG CCT AAC ATG CTT	MWG GmbH, Germany
	Probe	AAA GAA AGT CTT CAC TCT GCT GAA GGC ATC TCG	MWG GmbH, Germany
Interleukin-13	Forward	GCC CTC AGG GAG CTC ATT G	TIB MOLBIOL, Germany
	Reverse	TGC AGC CTG ACA CGT TGA TC	TIB MOLBIOL, Germany
	Probe	TCA ACA TCA CCC AGA ACC AGA AGG CTC	MWG GmbH, Germany
Interferon-γ	Forward	CAG GTC ATT CAG ATG TAG CGG ATA A	MWG GmbH, Germany
	Reverse	AGG AGA CAA TTT GGC TCT GCA TT	MWG GmbH, Germany
	Probe	TTT CTG TCA CTC TCC TCT TTC CAA TTC TTC AAA	MWG GmbH, Germany
Tumour necrosis factor-α	Forward	TCT CGA ACC CCG AGT GAC AA	MWG GmbH, Germany
	Reverse	TCA GCC ACT GGA GCT GCC	MWG GmbH, Germany
	Probe	TGT AGC CCA TGT TGT AGC AAA CCC TCA AGC	MWG GmbH, Germany
CX3CR1	Forward	TGA CTG GCA GAT CCA GAG GTT	MWG GmbH, Germany
	Reverse	TTC TGT CAC TGA TTC AGG GAA CTG	MWG GmbH, Germany
	Probe	AGT CCA CGC CAG GCC TTC ACC A	MWG GmbH, Germany

Table 2. Concentrations of used cytokines

	c1	c2	c3
Transforming growth factor-β	0·1 ng/ml	1 ng/ml	10 ng/ml
Interleukin-18	1 ng/ml	10 ng/ml	100 ng/ml
Interleukin-15	50 ng/ml	100 ng/ml	200 ng/ml
Interleukin-12	1 ng/ml	10 ng/ml	100 ng/ml
Interleukin-2	10 U/ml	50 U/ml	100 U/ml
Interleukin-21	10 ng/ml	30 ng/ml	100 ng/ml

5% CO_2 for 5 days. Afterwards proliferating NK cells were determined by flow cytometry.

Co-culture of monocytes and NK cells

Freshly isolated NK cells were sorted into CX3CR1$^{neg/low}$ and CX3CR1^{high} fractions and were adjusted to 1×10^6 per ml and used as effector cells. Freshly magnetically sorted monocytes were also adjusted to 1×10^6 per ml and used as target cells. Cells were plated at the ratio of 3 : 1 (effector : target cell) and incubated for 36 hr at 37° in 5% CO_2. Cultures with only monocytes served as a control. To facilitate the separation of monocytes from the plate after the culturing period, cells were incubated for 1 hr in ice-cold PBS in the refrigerator. Cells were than carefully harvested, washed with PBS and stored in FACS buffer (PBS containing 0·5% BSA; pH 7·2–7·4) for the subsequent flow cytometric analysis.

Statistical analysis

The Mann–Whitney *U*-test was used to calculate *P*-values for intergroup comparison of two groups for real-time RT-PCR data on cytokine profiles and flow cytometry data on CD25 expression. The Wilcoxon test was used to calculate *P*-values for real-time RT-PCR data on modulation of CX3CR1 by cytokines. The Kruskal–Wallis non-parametric one-way analysis of variance was performed to assess the relation between multiple groups. Specific associations between groups were assessed with the Mann–Whitney *U*-test for non-parametric data. Bonferroni–Holm corrections were also performed for multiple Mann–Whitney *U*-test comparisons. The calculations were carried out using SPSS 12.0 and 18.0 software for Windows (SPSS, Chicago, IL). A *P*-value of $< 0{\cdot}05$ was regarded as significant.

Results

Human CX3CR1$^{neg/low}$ and CX3CR1^{high} NK cells differ in their cytokine signature, activation status and proliferative response

To address whether the expression of CX3CR1 on human NK cells is associated with a certain cytokine profile and therefore with a particular function, we analysed the expression of cytokines such as interferon-γ (IFN-γ), tumour necrosis factor-α (TNF-α), GM-CSF, IL-5, IL-10 and IL-13 in CX3CR1$^{neg/low}$ and CX3CR1^{high} NK cell fractions. The NK cells were magnetically sorted from freshly isolated PBMCs and FACS-sorted into CX3CR1$^{neg/low}$ and CX3CR1^{high} fractions, incubated with mitogens (PMA/ionomycin), and analysed by quantitative real-time RT-PCR. CX3CR1$^{neg/low}$ NK cells expressed significantly higher amounts of IL-5, IL-10, IL-13, GM-CSF and TNF-α compared with CX3CR1^{high} NK cells (Fig. 1a). Compared with CX3CR1^{high}, CX3CR1$^{neg/low}$ NK cells expressed approximately 30 times more IL-5, up to 15 times more of the regulatory cytokine IL-10, about four times more TNF-α and more than twice as much GM-CSF. The expression of IL-13 was more than 100 times higher by CX3CR1$^{neg/low}$ than by CX3CR1^{high} NK cells. No differences were observed between the two fractions in the expression of IFN-γ (Fig. 1a).

To determine whether CX3CR1$^{neg/low}$ and CX3CR1^{high} NK cell populations may differ in their activation status, we analysed CD25 expression on both NK cell subsets in freshly isolated PBMCs using flow cytometric analysis. We measured a significantly higher expression of CD25 on CX3CR1$^{neg/low}$-expressing NK cells compared with their CX3CR1^{high} counterparts (Fig. 1b). As CD25 is the alpha subunit of the high-affinity IL-2 receptor, we questioned whether proliferative response to IL-2 may also differ between the CX3CR1$^{neg/low}$ and CX3CR1^{high} NK cell populations. To measure proliferation, NK cell subsets were sorted combining MACS and FACS sorting procedures. Sorted CX3CR1$^{neg/low}$ and CX3CR1^{high} cells were then incubated for 72 hr with and without recombinant IL-2. We observed a complete lack of response of CX3CR1^{high} NK cells to IL-2 whereas the CX3CR1$^{neg/low}$ fraction strongly proliferated in the presence of IL-2 (Fig. 1c).

CX3CR1$^{neg/low}$ and CX3CR1^{high} NK cells do not influence the phenotype of monocytes but differentially modulate their co-stimulatory capacities

To determine whether CX3CR1$^{neg/low}$ and CX3CR1^{high} NK cells are functionally distinct subsets, we investigated how these two subtypes influence T-cell proliferation and monocyte function *in vitro*. We performed proliferation assays with positively selected human CD4$^+$ T cells activated by anti-CD3/anti-CD28 antibodies in the presence of sorted autologous CX3CR1^{high} or CX3CR1$^{neg/low}$ NK cells in different ratios. There was no effect of either CX3CR1^{high} or CX3CR1$^{neg/low}$ NK cells on the proliferative T-cell response (data not shown). Yet, this does not exclude a possible distinct cytotoxic action of the NK cell fractions on autologous T cells. However, NK cell-mediated T-cell cytotoxicity could not be assessed because this can only be achieved using cytokine-activated NK cells[25,26] a pre-activa-

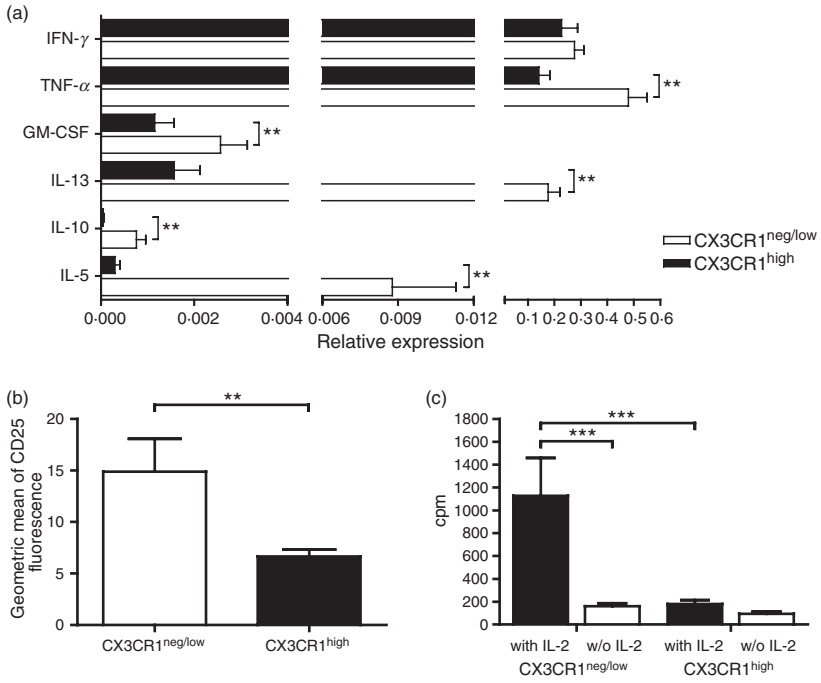

Figure 1. Human CX3CR1$^{neg/low}$ and CX3CR1^{high} natural killer (NK) cells show different pattern of cytokine expression, different levels of surface CD25 and different proliferative capacities. (a) Magnetically isolated NK cells were FACS-sorted into CX3CR1$^{neg/low}$ and CX3CR1^{high} fractions and incubated with mitogens (PMA/Ionomycin) for 4 hr. Gene expression of interferon-γ (IFN-γ), tumour necrosis factor-α (TNF-α), granulocyte–macrophage colony-stimulating factor (GM-CSF), interleukin-13 (IL-13), IL-10 and IL-5 of CX3CR1$^{neg/low}$ NK cells (white bar) compared with CX3CR1^{high} NK cells (shaded bar) was analysed using real-time RT-PCR. The data are normalized to the housekeeping gene *b-actin* and are expressed as the mean relative expression of at least four independent experiments ± SEM. $^{**}P < 0{\cdot}01$. (b) CD25 expression on CD56^{+} CD16^{+} CD3^{-} CX3CR1$^{neg/low}$ and CD56^{+} CD16^{+} CD3^{-} CX3CR1^{high} expressing cells was determined by flow cytometry. The *y*-axis shows the mean fluorescence intensity of the CD25 staining. The figure shows a higher expression of CD25 on CX3CR1$^{neg/low}$ NK cells compared with CX3CR1^{high} NK cells. Data from six independent experiments ± SEM are represented. $^{**}P < 0{\cdot}01$. (c) The figure shows the proliferative response to IL-2 of the CX3CR1$^{neg/low}$ and CX3CR1^{high} NK cell fractions. NK cells were incubated with or without IL-2 (100 U/ml) for 72 hr. Proliferation response was assessed by [^{3}H]thymidine uptake in triplicates and shown as the mean c.p.m. of four independent experiments ± SEM. Data show a strong IL-2-mediated proliferation of CX3CR1$^{neg/low}$ NK cells exclusively. $^{***}P < 0{\cdot}001$.

tion that, in turn, would affect the CX3CR1^{high} and CX3CR1$^{neg/low}$ phenotypes investigated here.

Next, we examined whether these NK cell subsets could differentially influence the phenotype and hence the antigen-presenting activity of human monocytes. The MACS-sorted monocytes were co-cultured with MACS/FACS-sorted autologous CX3CR1^{high} and CX3CR1$^{neg/low}$ NK cells in a 1 : 3 ratio. After 36 hr, the expression of CD14, HLA-DR, CD86 and CD40 was assessed on non-lymphocytic CD11c-positive cells using flow cytometry. Figure 2(a) shows that after 36 hr of co-incubation of NK cells/monocytes, neither CX3CR1^{high} nor CX3CR1$^{neg/low}$ NK cells affected the expression of the monocyte marker CD14. Hence, monocytes retain their phenotype after co-culturing with NK cells over a period of 36 hr and did not differentiate into dendritic cells. Furthermore, we found that both CX3CR1^{high} and CX3CR1$^{neg/low}$ induced down-regulation of CD86 expression and a slight decrease of HLA-DR on monocytes (Fig. 2b). Interestingly, in contrast to the CX3CR1^{high} fraction, CX3CR1$^{neg/low}$ NK cells promoted a 2·5-fold increase of CD40 expression (Fig. 2b), indicating that the CX3CR1$^{neg/low}$ NK cells differ from the CX3CR1^{high} subset in their ability to influence the co-stimulatory capacities of monocytes.

CX3CR1$^{neg/low}$ NK cells differ from the CD56^{bright} CD16^{-} subset

A few years ago, Cooper *et al.*[27] identified two distinct subsets of human NK cells based on different levels of expression of CD56. While CD56^{dim} CD16^{bright} NK cells (representing 90% of peripheral blood NK cells) primarily function as potent cytolytic effector cells, CD56^{bright} CD16$^{-/dim}$ NK cells represent a minor subset of poorly cytolytic NK cells that briskly secrete diverse cytokines such as IFN-γ, TNF-α or IL-10. The CX3CR1^{high} and CX3CR1$^{neg/low}$ populations appear to show similar features to the CD56^{dim} and CD56^{bright}, respectively, so we asked whether expression of the chemokine receptor and expression intensity of CD56 define the same NK cell subsets. Using conventional flow cytometric analysis, we confirmed that CX3CR1^{high} NK cells were CD56^{dim} NK

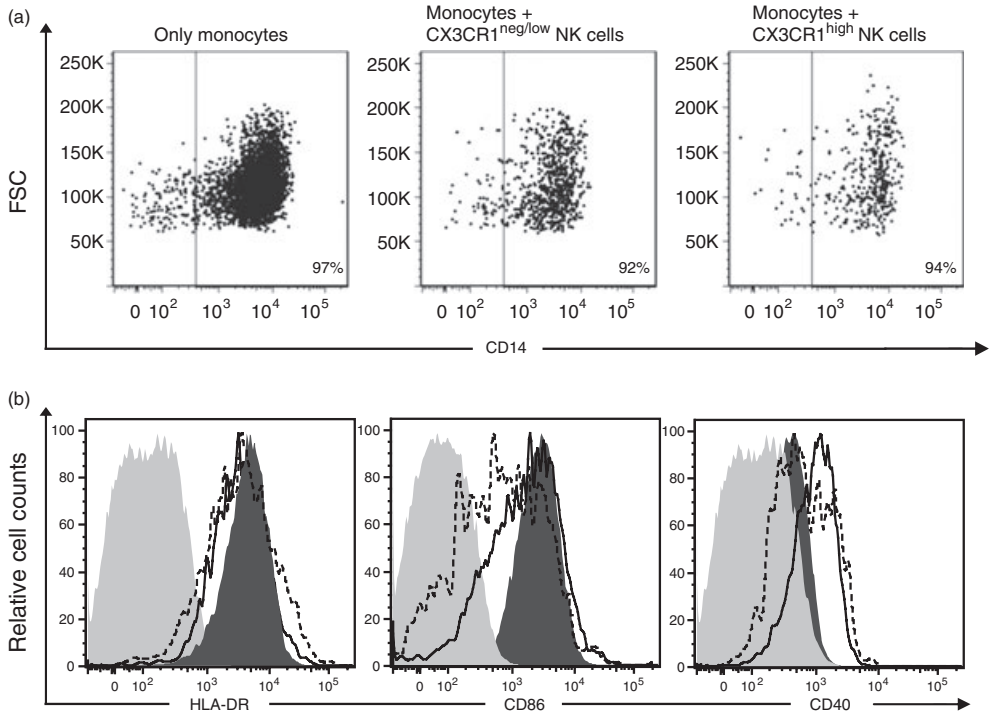

Figure 2. CX3CR1$^{neg/low}$ and CX3CR1^{high} natural killer (NK) cells do not modulate CD14 expression on monocytes but differentially influence monocytic co-stimulatory capacities. Sorted monocytes were incubated with autologous CX3CR1$^{negative/low}$ and CX3CR1^{high} for 36 hr. Expression of CD14, HLA-DR and co-stimulatory molecules CD86 and CD40 was analysed on CD11c-positive non-lymphocytic cells using flow cytometry. (a) The dot plots show that CD14 expression on monocytes remained unaffected after co-culture without or with CX3CR1$^{neg/low}$ and CX3CR1^{high} NK cells. (b) Histograms show the expression of the different markers/molecules on monocytes cultured without NK cells (filled dark grey histogram), after co-culturing with CX3CR1$^{neg/low}$ NK cells (solid line) and CX3CR1^{high} NK cells (dashed line). Control staining is shown as filled, light grey histograms. Data are representative of three independent experiments.

cells. However, we showed that CX3CR1$^{neg/low}$ NK cells encompassed not only all CD56^{bright} cells (CD16^{+} and CD16^{-}) but also a large subpopulation (up to 60%) of CD56^{dim} CD16^{bright} NK cells (Fig. 3a). It was important to exclude the possibility that the presence of CD56^{dim} cells in the CX3CR1$^{neg/low}$ fraction was not caused by inclusion in the analysis of cells expressing low amounts of CX3CR1. We therefore restricted our examination to NK cells that completely lacked CX3CR1 expression. We found that about 45% of the CX3CR1-negative cells were CD56^{dim} (Fig. 3b). These data indicate that CX3CR1$^{neg/low}$ NK cells include not only the classical immunomodulatory CD56^{bright} population but also a high percentage of CD56^{dim} cells. Hence, our data identified three distinct NK cell subsets based on their expression of CX3CR1 and CD56: CX3CR1^{neg} CD56^{bright}, CX3CR1^{neg} CD56^{dim} and CX3CR1^{high} CD56^{dim} NK cells. The analysis of the CD25 expression (Fig. 3c) and proliferative capacities in response to IL-2 measured by CFSE dilution assays (Fig. 3d) of these three populations indicated that CX3CR1^{neg} CD56^{dim} NK cells may represent an intermediary phenotype between CX3CR1^{neg} CD56^{bright} and CX3CR1^{high} CD56^{dim} NK cells. Notably, compared with the CX3CR1^{high} CD56^{dim} population, the CX3CR1^{neg} CD56^{dim} fraction strongly proliferated, indicating that lack of proliferative capacity may correlate better with the magnitude of CX3CR1 expression than with reduced density of CD56 expression.

Degree of CX3CR1 expression defines different maturation stages of CD56^{dim} NK cells

To further characterize the distinct CX3CR1^{neg} CD56^{bright}, CX3CR1^{neg} CD56^{dim} and CX3CR1^{high} CD56^{dim} NK cell fractions, we assessed the expression of killer cell immunoglobulin-like receptors (KIR, including KIR2DL1/2DS1/2DL2/2DS2/2DL3/3DL1/3DL2/3DS1), NKG2A and NKp30 and NKp46 on these three NK cell populations using flow cytometry (Fig. 4a). The majority of CX3CR1^{neg} CD56^{bright} NK cells did not express KIR on the surface; however, more than 95% of these NK cells were high expressers of NKp30 and NKp46, and about 80% expressed high levels of NKG2A. In all samples investigated, the grade of CX3CR1 expression in the CD56^{dim} NK cell fraction coincided with a decrease in the expression of NKp30, NKp46 and NKG2A and with an increased KIR expression (Fig. 4a). Hence, CX3CR1^{neg} CD56^{dim} NK cells appear to represent a phenotypic stage

between proliferating, cytokine-producing NKG2A/NKp30/NKp46-expressing NK cells and non-proliferating KIR-expressing NK cells.

As the expression of CD27, CD62L and CD57 has been shown to characterize different steps of NK cell maturation,[28–31] we addressed how CX3CR1 expression is related

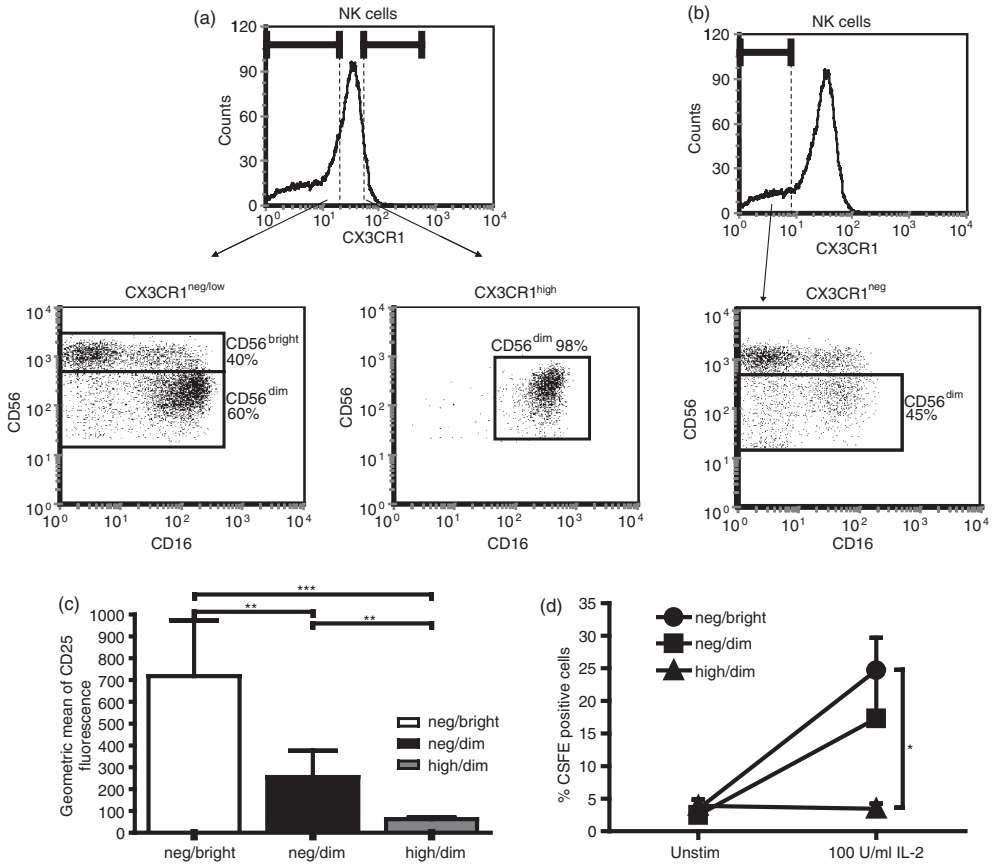

Figure 3. CX3CR1$^{neg/low}$ natural killer (NK) cells encompass a CD56^{bright} and a CD56^{dim} NK cell fraction. (a) CD56 expression on CX3CR1$^{neg/low}$ and CX3CR1^{high} NK cells was determined using flow cytometry. The dot plots demonstrate that about 40% of all CX3CR1$^{neg/low}$ cells were CD56^{bright} while 60% were CD56^{dim}. Almost all CX3CR1^{high} cells were CD56^{dim}. (b) From the CX3CR1^{neg} NK cells, about 45% were CD56^{dim}. Hence, gating on CX3CR1^{neg} and CX3CR1^{high} cells, three NK cell fractions can be defined based on CD56 expression: CX3CR1^{neg} CD56^{bright}, CX3CR1^{neg} CD56^{dim} and CX3CR1^{high} CD56^{dim} NK cells. Data are representative of four independent experiments. (c) CD25 expression on CX3CR1^{neg} CD56^{bright} (neg/bright), CX3CR1^{neg} CD56^{dim} (neg/dim) and CX3CR1^{high} CD56^{dim} (high/dim) was determined in freshly isolated peripheral blood mononucelar cells (PBMCs). Flow cytometric analyses revealed CX3CR1^{neg} CD56^{dim} as an intermediary phenotype (black bar), which showed an intermediate significantly distinct expression of CD25 when compared with neg/bright-expressing NK cells (white bar) and high/dim-expressing NK cells (grey bar). The data are normalized to *b-actin* and are shown as the mean relative expression of 11 independent experiments ± SEM. $^{*}P < 0{\cdot}05$. (d) Proliferative capacity of CX3CR1^{neg} CD56^{bright}, CX3CR1^{neg} CD56^{dim} and CX3CR1^{high} CD56^{dim} NK cell fractions was measured by CSFE dilution after 5 days of stimulation with or without 100 U/ml interleukin-2 (IL-2). CX3CR1^{neg} CD56^{bright} (neg/bright) and CX3CR1^{neg} CD56^{dim} (neg/dim) NK cells proliferate strongly in the presence of IL-2, whereas no proliferation was detected in the CX3CR1^{high} CD56^{dim} (high/dim) fraction. The data are shown as the mean percentage of proliferating cells of eight independent experiments ± SEM. $^{*}P < 0{\cdot}05$

Figure 4. CX3CR1^{neg} CD56^{bright}, CX3CR1^{neg} CD56^{dim} and CX3CR1^{high} CD56^{dim} natural killer (NK) cells show different patterns of NK cell receptors and maturation markers. (a) NK cell receptor expression on the three NK cell subsets was determined by flow cytometry. CX3CR1^{neg} CD56^{dim} (neg/dim) show an intermediate expression of NKp30, NKp46, NKG2A and KIR2DL1/2DS1/2DL2/2DS2/2DL3/3DL1/3DL2/3DS1 (indicated as panKIR) compared with neg/bright and high/dim-expressing NK cells. Data from at least 10 independent experiments are shown. $^{**}P < 0{\cdot}01$, $^{***}P < 0{\cdot}001$. (b) The panel shows flow cytometric analysis of peripheral blood mononuclear cells stained for CD62L, CD57 and CD27, gated first for CD3^{-} CD56^{+} CD16^{+} cells and gated subsequently for CX3CR1^{neg} CD56^{bright} (neg/bright), CX3CR1^{neg} CD56^{dim} (neg/dim) and CX3CR1^{high} CD56^{dim} (high/dim) NK cells. The figures are representative of at least 13 independent donors. (c) Percentage of CD62L-, CD57- and CD27-expressing in CX3CR1^{neg} CD56^{bright} (neg/bright), CX3CR1^{neg} CD56^{dim} (neg/dim) and CX3CR1^{high} CD56^{dim} (high/dim) NK cells was determined using flow cytometry. Data of at least 13 independent experiments and representative dot plots are shown. $^{**}P < 0{\cdot}01$, $^{***}P < 0{\cdot}001$.

to the expression of these recently identified maturation markers. We monitored the surface expression of CD27, CD62L and CD57 on CX3CR1^{neg} CD56^{bright}, CX3CR1^{neg} CD56^{dim} and CX3CR1^{high} CD56^{dim} NK cells using flow cytometry. The majority of CX3CR1^{neg} CD56^{bright} NK cells expressed CD27 and CD62L and were negative for CD57. However, in the CX3CR1^{neg} CD56^{dim}, we observed a strong reduction of CD27 and CD62L, and increased expression of CD57. Interestingly, although the expression of CD57 did not differ between CX3CR1^{neg} CD56^{dim} and

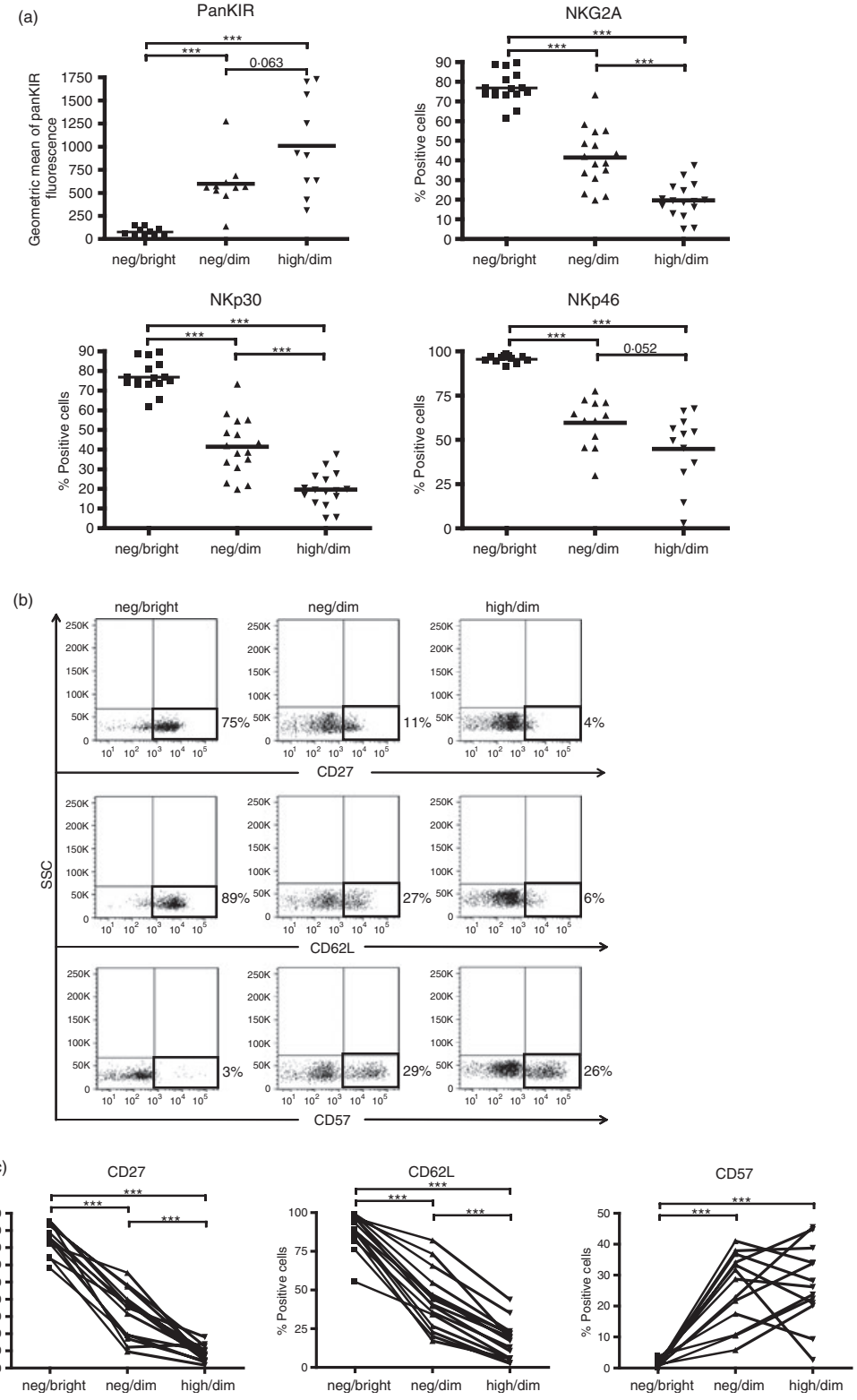

CX3CR1^{high} CD56^{dim} NK cells, both CD27 and CD62L expression were further decreased in the CX3CR1^{neg} CD56^{dim} fraction when compared with the CX3CR1^{high} CD56^{dim} population (Fig. 4b,c).

Hence, the expression pattern of CD27 and CD62L on CX3CR1^{neg} CD56^{bright}, CX3CR1^{neg} CD56^{dim} and CX3CR1^{high} CD56^{dim} NK cells indicates that these three phenotypes indeed reflect distinct stages of NK cell maturation. Additional studies combining analysis of CX3CR1 expression with other NK cell markers are needed to establish and understand the sequential stages of NK cell differentiation.

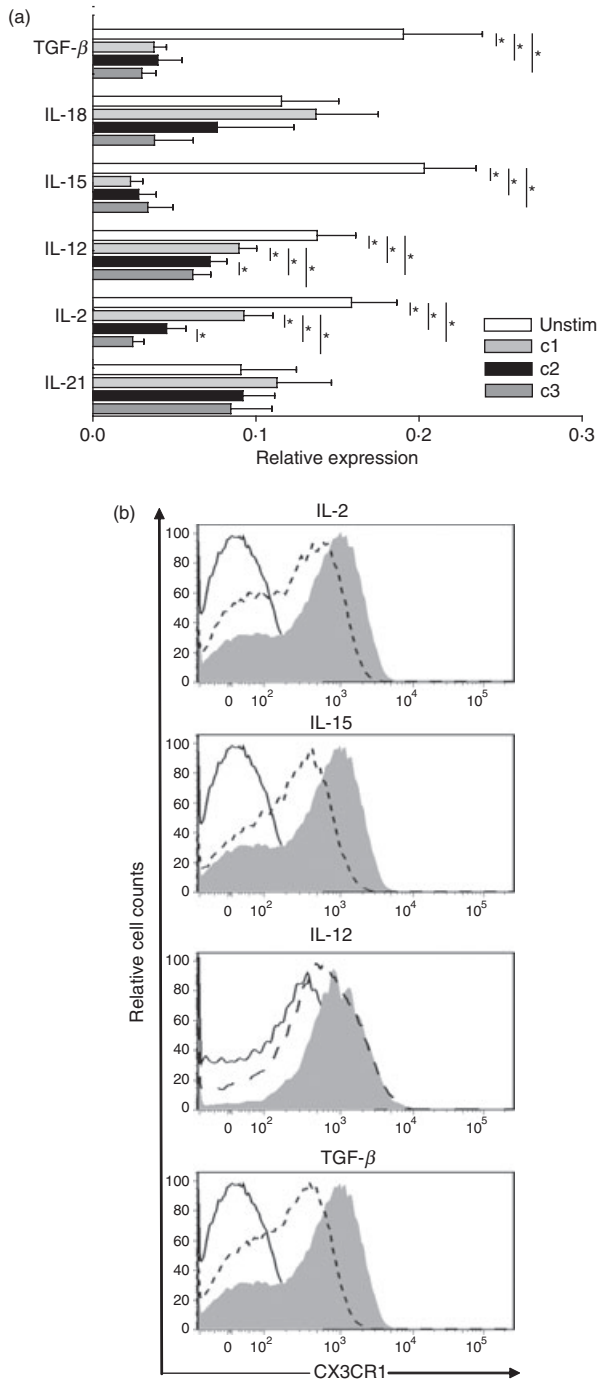

Cytokines responsible for NK cell activation induce down-regulation of CX3CR1 expression

We previously showed that the frequency of CX3CR1-expressing NK cells correlated with disease activity of multiple sclerosis.[24] However, to understand the relationship between pathology and degree of receptor expression, additional information on CX3CR1 regulation is required. We address here the question of how the immune milieu may influence CX3CR1 expression on NK cells. We assessed the effect on CX3CR1 of different cytokines known to modulate NK cell activity, including the related cytokines IL-2, IL-15 and IL-21, the IFN-γ-inducing cytokines IL-12 and IL-18 as well as the inhibitory cytokine TGF-β. CX3CR1 gene expression was quantified by real-time RT-PCR. Negatively selected resting NK cells were incubated for 20–22 hr with different cytokine concentrations (see Table 2). Our data showed that while IL-2 and IL-15 induced a strong down-regulation of CX3CR1 in a concentration-dependent way, IL-21 had no effect (Fig. 5a). Both IL-12 and TGF-β1 also promoted a concentration-dependent down-regulation CX3CR1 expression (Fig. 5a). Data for IL-18 showed a trend towards CX3CR1 down-regulation but did not reach statistical significance. Next, we investigated the effects of the most relevant cytokines, IL-2, IL-15, IL-12 and TGF-β on the surface expression of CX3CR1. Magnetically sorted NK cells were stimulated for 24 hr without any additives, or in the presence of IL-2 (100 U/ml), IL-15 (200 ng/ml), IL-12 (100 ng/ml) and TGF-β (10 ng/ml), respectively. CX3CR1 expression was analysed using flow cytometry. The protein data confirmed the observation on gene expression levels, showing a cytokine-dependent down-regulation of surface CX3CR1 on NK cells (Fig. 5b).

Figure 5. Natural killer (NK) cell-activating cytokines induce down-regulation of CX3CR1 expression. The NK cells were cultured without or in the presence of different concentrations of the indicated cytokines for 20–22 hr (see Table 2 for cytokine concentrations). (a) Expression of CX3CR1 was determined by quantitative real-time RT-PCR. The data are normalized to the housekeeping gene *beta-actin*, and are expressed as the mean relative expression of at least four independent experiments ± SEM. Interleukin-2 (IL-2), IL-12, IL-15 and transforming growth factor-β (TGF-β) promoted a significant dose-dependent down-regulation of the receptor. Down-regulation of CX3CR1 promoted by IL-18 did not reach statistical significance and IL-21 did not show any effect on CX3CR1 expression. *$P < 0{\cdot}05$. (b) Expression of surface CX3CR1 on NK cells was monitored using flow cytometry. Solid lines represent unstained controls; shaded areas, unstimulated NK cells; dashed lines, NK cells stimulated with the highest concentration of the respective cytokines (100 U/ml IL-2; 200 ng/ml IL-15; 100 ng/ml IL-12; 10 ng/ml TGF-β). One representative experiment of at least three is shown.

Moreover, the strongest CX3CR1 down-regulation was observed in the presence of IL-15 and TGF-β, which also confirmed data obtained by PCR. Hence, most cytokines inducing activation/proliferation of NK cells negatively influence CX3CR1 expression, indicating a dynamic relation between CX3CR1^{high} and CX3CR1$^{neg/low}$ subsets.

Discussion

In our previous study, we observed an association between the expression of CX3CR1 on NK cells and multiple sclerosis. To further elucidate the involvement of CX3CR1-expressing NK cells in disease, we aimed here to characterize the phenotype and functionality of CX3CR1^{high} and CX3CR1$^{neg/low}$ NK cell populations. We demonstrated that CX3CR1^{high} and CX3CR1$^{neg/low}$ NK cell phenotypes are distinct from the NK1/NK2 or CD56^{dim} CD56^{bright} NK cells, two NK cell pairs identified previously.[27,32,33] Similarly to NK2 cells, CX3CR1$^{neg/low}$ NK cells expressed high levels of IL-5 and IL-13, but also of IL-10 (Fig. 1), shown to be produced by NK1 cells.[32] Furthermore, CX3CR1$^{neg/low}$ NK cells expressed similar amounts of IFN-γ but significantly more GM-CSF and TNF-α than CX3CR1^{high} (Fig. 1a), hence differing also from the cytokine profile of CD56^{bright} CD56^{dim} subsets. Furthermore, we showed a high expression of the activation marker CD25 on CX3CR1$^{neg/low}$ NK cells (Fig. 1b), which was accompanied by a very strong proliferative response to IL-2 *in vitro* (Fig. 1c).

Next, we asked to what extent CX3CR1^{high} and CX3CR1$^{neg/low}$ NK cell subsets could differentially affect the adaptive immune response. In our experiments, human NK cells, independent of their CX3CR1 expression, were unable to influence proliferation of autologous activated T cells (data not shown) but modulated the co-stimulatory capacities of monocytes (Fig. 2b) without affecting monocytic phenotype (Fig. 2a). In this approach, we did not activate NK cells with either IL-2 or IL-15 to exclude the possible effects of these cytokines on CX3CR1^{high} and CX3CR1$^{neg/low}$ phenotypes. We showed that after 36 hr of co-culturing both CX3CR1^{high} and CX3CR1$^{neg/low}$ NK cells induced down-regulation of CD86 and HLA-DR on monocytes, whereas up-regulation of CD40 was induced principally by CX3CR1$^{neg/low}$ NK cells (Fig. 2b). This is in agreement with the results by Zhang *et al.*[34] who recently reported the up-regulation of CD40 on monocytes co-cultured with NK cells, especially CD56^{bright} NK cells. Yet 36 hr of co-culturing was obviously too short for observing possible differentiation of monocytes into dendritic cells as reported previously.[34] The CX3CR1$^{neg/low}$ NK cell fraction parallels CD56^{bright} NK cells, in terms of both proliferative capacities[35] and monocyte modulation. However, the analysis of the co-expression of CD56 and CX3CR1 revealed that while all CX3CR1^{high} NK cells were indeed CD56^{dim} CD16^{high}, the CX3CR1$^{neg/low}$ fraction encompassed both CD56^{dim} CD16^{low} and CD56^{bright} CD16$^{neg/low}$ NK cells (Fig. 3a). Our data suggest the existence of distinct NK cell populations based on CD56 and CX3CR1 expression: CX3CR1^{neg} CD56^{bright}, CX3CR1^{neg} CD56^{dim} and CX3CR1^{high} CD56^{dim} NK cells. Interestingly, the analysis of surface CD25 expression and of the proliferative response indicated that these three fractions represented distinct NK cell phenotypes (Fig. 3c,d). These findings were also confirmed by examination of the expression of different NK receptors on CX3CR1^{neg} CD56^{bright}, CX3CR1^{neg} CD56^{dim} and CX3CR1^{high} CD56^{dim} NK cells. All the analysed receptors showed a similar expression pattern, progressively increasing for KIR and gradually decreasing for NKp30, NKp46 and NKG2A from CX3CR1^{neg} CD56^{bright} to CX3CR1^{high} CD56^{dim} (Fig. 4a). These data verified that CX3CR1^{neg} CD56^{dim} NK cells indeed represent an intermediate phenotype distinct from the CX3CR1^{high} CD56^{dim} subset. Several recent publications have reported on markers characterizing different stages of NK cell maturation, including CD27,[28] CD94,[36] CD62L[29] and CD57.[30,31] Expression analysis of CD27, CD62L and CD57 on CX3CR1^{neg} CD56^{bright}, CX3CR1^{neg} CD56^{dim} and CX3CR1^{high} CD56^{dim} NK cells showed that, from the fractions investigated here, only the CX3CR1^{high} CD56^{dim} subset parallels the mature phenotype as defined by the lack of CD27 and CD62L and the acquisition of CD57 (Fig. 4b,c). According to our previous data,[24] we focused here on different NK cell fractions selected on the basis of the magnitude of CX3CR1 expression (CX3CR1^{neg} and CX3CR1^{high}). Even though our data indicate that the whole CX3CR1-positive fraction has a similar phenotype to CX3CR1^{high}-expressing NK cells, further analyses are needed to demonstrate this equivalence.

Interestingly, with regards to CD57 expression, the intermediary CX3CR1^{neg} CD56^{dim} fraction appears to encompass different stages of differentiation. Additional investigations of this intermediate population will be needed to determine whether the CX3CR1^{neg} CD56^{dim} CD57^{-} phenotype may differ from the CX3CR1^{neg} CD56^{dim} CD57^{+}.

Moreover, we present here evidence for cytokine-mediated regulation of CX3CR1 in NK cells. We showed that not only IL-15, but also IL-2 down-regulated CX3CR1 expression on human NK cells at the RNA (Fig. 5a) and protein (Fig. 5b) levels. Although they may contradict the murine data published so far,[37] our results are in agreement with the identical effects of these structurally related cytokines on human resting NK cells observed by Dunne *et al.*[38] In mice, it has been reported that whereas IL-2 induces increased expression of CX3CR1 on NK cells, IL-15 down-regulated the receptor expression despite their structural similarities. No effect was observed when NK cells were stimulated with IL-21 (Fig. 5a), although this cytokine shares the gamma-chain of the receptor, among others, with IL-2 and IL-15.[39] It is possible that IL-21

affects CX3CR1 expression only in synergy with other cytokines, as was also reported for other effects of IL-21 on NK cell biology.[40,41] We also observed a down-regulation of CX3CR1 gene and protein expression on NK cells induced by TGF-β (Fig. 5a,b), which, on the one hand, appeared to contradict the effects reported in rats[42] but, on the other hand, were consistent with the reported inhibitory effects of TGF-β on human NK cells.[43,44] Hence, a different regulation of NK cell function and CX3CR1 expression in rodents and humans seems to be probable. Similarly, we observed a down-regulation of CX3CR1 expression by IL-12, an additional cytokine involved in NK cell immunomodulation,[45] suggesting that most cytokines known to induce NK cell proliferation/activation promote CX3CR1 down-regulation.

In summary, our data show the existence of distinct NK cell phenotypes depending on the magnitude of CX3CR1 expression. The NK cell phenotypes defined by CX3CR1 expression differ in their cytolytic activity, cytokine profile, proliferative response and their impact on monocyte functionality. Moreover, we identified three different stages of NK cell maturation based on the expression of CX3CR1 and CD56. While the CX3CR1^{neg} CD56^{bright} phenotype is exclusively characteristic for immature NK cells, the magnitude of CX3CR1 expression on CD56^{dim} NK cells discriminates between intermediary CX3CR1^{neg} CD56^{dim} and fully mature CX3CR1^{high} CD56^{dim} NK cells. Hence, our study demonstrates that CX3CR1 can be used in conjunction with CD56 and with other novel maturation markers to delineate NK cell phenotypes characteristic for the sequential stages of human NK cell maturation.

Acknowledgements

This work was supported by grants from the Charité (Rahel-Hirsch Stipend to C.I-D.), the Graduate Research School GRK1258 and the German Research Council (SFB 650). We thank Bibiane Seeger and Thordis Hohnstein for excellent technical support, Alexander Brandt for help with the statistical analyses, Lena Mann for reading the manuscript as a native English speaker and Jason Millward for critical reading of the manuscript.

Disclosures

The authors have no conflict of interest.

References

1 Cardona AE, Ransohoff RM. Chemokine receptor CX3CR1. *UCSD-Nat Mol Pages* 2009; doi:10.1038/mp.a000633.01.

2 Fraticelli P, Sironi M, Bianchi G *et al.* Fractalkine (CX3CL1) as an amplification circuit of polarized Th1 responses. *J Clin Invest* 2001; **107**:1173–81.

3 Nishimura M, Umehara H, Nakayama T *et al.* Dual functions of fractalkine/CX3C ligand 1 in trafficking of perforin$^+$/granzyme B$^+$ cytotoxic effector lymphocytes that are defined by CX3CR1 expression. *J Immunol* 2002; **168**:6173–80.

4 Dichmann S, Herouy Y, Purlis D, Rheinen H, Gebicke-Harter P, Norgauer J. Fractalkine induces chemotaxis and actin polymerization in human dendritic cells. *Inflamm Res* 2001; **50**:529–33.

5 Moatti D, Faure S, Fumeron F *et al.* Polymorphism in the fractalkine receptor CX3CR1 as a genetic risk factor for coronary artery disease. *Blood* 2001; **97**:1925–8.

6 McDermott DH, Halcox JP, Schenke WH, Waclawiw MA, Merrell MN, Epstein N, Quyyumi AA, Murphy PM. Association between polymorphism in the chemokine receptor CX3CR1 and coronary vascular endothelial dysfunction and atherosclerosis. *Circ Res* 2001; **89**:401–7.

7 Landsman L, Bar-On L, Zernecke A *et al.* CX3CR1 is required for monocyte homeostasis and atherogenesis by promoting cell survival. *Blood* 2009; **113**:963–72.

8 Tuo J, Smith BC, Bojanowski CM, Meleth AD, Gery I, Csaky KG, Chew EY, Chan CC. The involvement of sequence variation and expression of CX3CR1 in the pathogenesis of age-related macular degeneration. *FASEB J* 2004; **18**:1297–9.

9 Tuo J, Bojanowski CM, Zhou M *et al.* Murine ccl2/cx3cr1 deficiency results in retinal lesions mimicking human age-related macular degeneration. *Invest Ophthalmol Vis Sci* 2007; **48**:3827–36.

10 Simeoni E, Vassalli G, Seydoux C, Ramsay D, Noll G, von Segesser LK, Fleury S. CCR5, RANTES and CX3CR1 polymorphisms: possible genetic links with acute heart rejection. *Transplantation* 2005; **80**:1309–15.

11 Cao G, Lu Y, Gao R, Xin Y, Teng D, Wang J, Li Y. Expression of fractalkine, CX3CR1, and vascular endothelial growth factor in human chronic renal allograft rejection. *Transplant Proc* 2006; **38**:1998–2000.

12 Umehara H, Tanaka M, Sawaki T *et al.* Fractalkine in rheumatoid arthritis and allied conditions. *Mod Rheumatol* 2006; **16**:124–30.

13 Murphy G, Caplice N, Molloy M. Fractalkine in rheumatoid arthritis: a review to date. *Rheumatology (Oxford)* 2008; **47**:1446–51.

14 Bolovan-Fritts CA, Spector SA. Endothelial damage from cytomegalovirus-specific host immune response can be prevented by targeted disruption of fractalkine-CX3CR1 interaction. *Blood* 2008; **111**:175–82.

15 Soriano SG, Amaravadi LS, Wang YF *et al.* Mice deficient in fractalkine are less susceptible to cerebral ischemia-reperfusion injury. *J Neuroimmunol* 2002; **2**:59–65.

16 Sunnemark D, Eltayeb S, Nilsson M, Wallstrom E, Lassmann H, Olsson T, Berg AL, Ericsson-Dahlstrand A. CX3CL1 (fractalkine) and CX3CR1 expression in myelin oligodendrocyte glycoprotein-induced experimental autoimmune encephalomyelitis: kinetics and cellular origin. *J Neuroinflammation* 2005; **2**:17.

17 Mizuno T, Kawanokuchi J, Numata K, Suzumura A. Production and neuroprotective functions of fractalkine in the central nervous system. *Brain Res* 2003; **2**:65–70.

18 Cardona AE, Pioro EP, Sasse ME *et al.* Control of microglial neurotoxicity by the fractalkine receptor. *Nat Neurosci* 2006; **9**:917–24.

19 Huang D, Shi FD, Jung S *et al.* The neuronal chemokine CX3CL1/fractalkine selectively recruits NK cells that modify experimental autoimmune encephalomyelitis within the central nervous system. *FASEB J* 2006; **20**:896–905.

20 Infante-Duarte C, Waiczies S, Wuerfel J, Zipp F. New developments in understanding and treating neuroinflammation. *J Mol Med* 2008; **86**:975–85.

21 Zipp F, Aktas O. The brain as a target of inflammation: common pathways link inflammatory and neurodegenerative diseases. *Trends Neurosci* 2006; **29**:518–27.

22 Morandi B, Bramanti P, Bonaccorsi I, Montalto E, Oliveri D, Pezzino G, Navarra M, Ferlazzo G. Role of natural killer cells in the pathogenesis and progression of multiple sclerosis. *Pharmacol Res* 2008; **57**:1–5.

23 Flodstrom-Tullberg M, Bryceson YT, Shi FD, Hoglund P, Ljunggren HG. Natural killer cells in human autoimmunity. *Curr Opin Immunol* 2009; **21**:634–40.

24 Infante-Duarte C, Weber A, Kratzschmar J *et al.* Frequency of blood CX3CR1-positive natural killer cells correlates with disease activity in multiple sclerosis patients. *FASEB J* 2005; **19**:1902–4.

25 Molinero LL, Domaica CI, Fuertes MB, Girart MV, Rossi LE, Zwirner NW. Intracellular expression of MICA in activated CD4 T lymphocytes and protection from NK cell-mediated MICA-dependent cytotoxicity. *Hum Immunol* 2006; **67**:170–82.

26 Cerboni C, Zingoni A, Cippitelli M, Piccoli M, Frati L, Santoni A. Antigen-activated human T lymphocytes express cell-surface NKG2D ligands via an ATM/ATR-dependent mechanism and become susceptible to autologous NK- cell lysis. *Blood* 2007; **110**:606–15.

27 Cooper MA, Fehniger TA, Turner SC, Chen KS, Ghaheri BA, Ghayur T, Carson WE, Caligiuri MA. Human natural killer cells: a unique innate immunoregulatory role for the CD56^{bright} subset. *Blood* 2001; **97**:3146–51.

28 Vossen MT, Matmati M, Hertoghs KM *et al.* CD27 defines phenotypically and functionally different human NK cell subsets. *J Immunol* 2008; **180**:3739–45.

29 Juelke K, Killig M, Luetke-Eversloh M *et al.* CD62L expression identifies a unique subset of polyfunctional CD56^{dim} NK cells. *Blood* 2010; **116**:1299–307.

30 Bjorkstrom NK, Riese P, Heuts F *et al.* Expression patterns of NKG2A, KIR, and CD57 define a process of CD56^{dim} NK-cell differentiation uncoupled from NK-cell education. *Blood* 2010; **116**:3853–64.

31 Lopez-Verges S, Milush JM, Pandey S *et al.* CD57 defines a functionally distinct population of mature NK cells in the human $CD56^{dim}$ $CD16^{+}$ NK-cell subset. *Blood* 2010; **116**:3865–74.
32 Peritt D, Robertson S, Gri G, Showe L, Aste-Amezaga M, Trinchieri G. Differentiation of human NK cells into NK1 and NK2 subsets. *J Immunol* 1998; **161**:5821–4.
33 Cooper MA, Fehniger TA, Caligiuri MA. The biology of human natural killer-cell subsets. *Trends Immunol* 2001; **22**:633–40.
34 Zhang AL, Colmenero P, Purath U *et al.* Natural killer cells trigger differentiation of monocytes into dendritic cells. *Blood* 2007; **110**:2484–93.
35 Carson WE, Fehniger TA, Caligiuri MA. $CD56^{bright}$ natural killer cell subsets: characterization of distinct functional responses to interleukin-2 and the c-kit ligand. *Eur J Immunol* 1997; **27**:354–60.
36 Yu J, Mao HC, Wei M *et al.* CD94 surface density identifies a functional intermediary between the $CD56^{bright}$ and $CD56^{dim}$ human NK-cell subsets. *Blood* 2010; **115**:274–81.
37 Barlic J, Sechler JM, Murphy PM. IL-15 and IL-2 oppositely regulate expression of the chemokine receptor CX3CR1. *Blood* 2003; **102**:3494–503.
38 Dunne J, Lynch S, O'Farrelly C, Todryk S, Hegarty JE, Feighery C, Doherty DG. Selective expansion and partial activation of human NK cells and NK receptor-positive T cells by IL-2 and IL-15. *J Immunol* 2001; **167**:3129–38.
39 Habib T, Nelson A, Kaushansky K. IL-21: a novel IL-2-family lymphokine that modulates B, T, and natural killer cell responses. *J Allergy Clin Immunol* 2003; **112**:1033–45.
40 Parrish-Novak J, Foster DC, Holly RD, Clegg CH. Interleukin-21 and the IL-21 receptor: novel effectors of NK and T cell responses. *J Leukoc Biol* 2002; **72**:856–63.
41 de Rham C, Ferrari-Lacraz S, Jendly S, Schneiter G, Dayer JM, Villard J. The proinflammatory cytokines IL-2, IL-15 and IL-21 modulate the repertoire of mature human natural killer cell receptors. *Arthritis Res Ther* 2007; **9**:R125.
42 Chen S, Luo D, Streit WJ, Harrison JK. TGF-β_1 upregulates CX3CR1 expression and inhibits fractalkine-stimulated signaling in rat microglia. *J Neuroimmunol* 2002; **2**:46–55.
43 Bellone G, Aste-Amezaga M, Trinchieri G, Rodeck U. Regulation of NK cell functions by TGF-β1. *J Immunol* 1995; **155**:1066–73.
44 Rook AH, Kehrl JH, Wakefield LM, Roberts AB, Sporn MB, Burlington DB, Lane HC, Fauci AS. Effects of transforming growth factor beta on the functions of natural killer cells: depressed cytolytic activity and blunting of interferon responsiveness. *J Immunol* 1986; **136**:3916–20.
45 Agaugue S, Marcenaro E, Ferranti B, Moretta L, Moretta A. Human natural killer cells exposed to IL-2, IL-12, IL-18, or IL-4 differently modulate priming of naive T cells by monocyte-derived dendritic cells. *Blood* 2008; **112**:1776–83.